Characterizing exposure conditions for a quantum dot exposure chamber

Nicholas Clark

A thesis

submitted in partial fulfillment of the

requirements for the degree of

Master of Science

University of Washington

2012

Committee:

Mike Yost

Tim Gould

Tim Larson

Program Authorized to Offer Degree:

Environmental and Occupational Health Science - Public Health

Abstract

Nanotechnology holds promise as an emerging technology with myriad applications. For example, quantum dots (often abbreviated to Qdots) are a nanomaterial that can be used in anti-counterfeiting ink, photovoltaics, and biological imaging. However, the composition of Qdots raises an issue of particular relevance to the last application: in one ubiquitous formulation, their core contains cadmium, a potent toxicant. If the quantum dot's shell is destroyed by conditions inside the body, cadmium would be free to cause adverse effects. This leads to the necessity of assessing the potential cadmium toxicity of this type of Qdot.

Since workers that deal with these materials in particular are exposed by a number of routes, characterization of those distinct routes is imperative. This project deals with inhalation exposures, culminating in an apparatus that generates a Qdot-containing test atmosphere in a small chamber. By putting test organisms in this chamber, the extent of toxicological and biotransformational effects can be measured. The main purpose of this thesis project is to create the exposure system and characterize the quantum dot aerosol, through describing the number concentration, size distribution and the resulting dose of cadmium for a hypothetical test animal.

Introduction

Quantum dots are a promising type of nanomaterial. They are semiconductor crystals with (generally) cadmium selenide cores and zinc sulfide shells that improve performance and stability. By modifying the diameter of the core, it is possible to change the wavelength of light at which they fluoresce; this property makes them useful for biomedical imaging. The main methods of characterizing them are X-ray photoelectron spectroscopy, transmission electron microscopy and optical absorption (Hines & Guyot, 1996).

Due to the toxicity of cadmium, however, there is concern about the safety of using Qdots in actual medical applications. While initial studies found no cytotoxicity, they were mostly performed with cell lines that were resistant to the ill effects of heavy metals. Later studies showed that oxidation by air and UV light could cause the crystals to release cadmium, which caused toxicity in the cells as expected from normal heavy metal dosing (Derfus et al., 2003). Despite this, quantum dots have advantages over current types of fluorophores. The range of wavelength of light that can excite them is wide while the emitted wavelength can be precisely controlled, and their useful lifetime is longer than dyes that may bleach after fluorescing for only a few minutes (Jamieson et al., 2007). They can be further coated with various ligands such as trioctylphosphine oxide (TOPO) to facilitate biomedical applications and reduce cytotoxicity. Additionally, using a thick coating would significantly affect the particle's size, and

therefore its deposition. Indeed, only by using surface coating is it possible for Qdots to deliver targeted drugs or bind to specific types of cells. As long as the structure doesn't degrade, exposing the core, the type of coating determines the surface properties of the particle and remains one of the most important factors to consider in regards to interaction between the Qdot and its environment.

Still, coating the dots isn't a perfect solution. The reduced cytotoxicity may in fact only be due to cell-specific issues like differences in uptake of the particles rather than any reduction of the hazard of the quantum dot itself. This is complicated by the fact that a handful of core/cap/coating properties affect toxicity in multiple pathways. Besides reactions on the surface of the crystal releasing cadmium ions into the organism, toxic effects may also be the result of free radical formation and interaction between cellular components and the dots themselves. Finally, ligands attached to the surface of the dots to reduce the desorption of cadmium may have toxic effects on their own; for example, TOPO has been shown to damage DNA in cells in the absence of quantum dots (Ibid.). As such, it is important to balance the utility of this technology with effective risk management, and in order to accomplish that, methods of systematically examining the hazards of exposure must be developed.

The most feasible way for quantum dots to be delivered to the body involves them being placed into a solution that would not be rejected

outright—for example, saline. While quantum dots on their own could be used in delivery, using a carrier medium inhibits the formation of larger aggregates of dots. This is an issue for aerosols in general, but nanoparticles show a marked propensity to cling together (Hinds, 1999). Such aggregation would drastically reduce the particles' surface area, and consequently affect any biochemical activity.

Deliberate injection of Qdots is the route of exposure in medical imaging, but inhalation exposure is possible in most other applications. Naturally, since it is controlled by the administrator, injection doesn't require investigation into exposure characterization. However, inhalation does. To be able to correlate data on toxic effects in the respiratory tract with exposures in the real world, it is first necessary to simulate such exposures with a well-characterized, consistent method.

Several methods of generating specific test atmospheres for the purpose of nanotoxicology inhalation studies exist. There are two general categories: systems that generate an aerosol from a dry bulk powder of the nanomaterial under consideration, and systems that generate an aerosol from a suspension of the nanomaterial in a liquid. The first group generally uses a mechanical process(shearing, acoustic energy, vibration, etc.) to deagglomerate the dry particles and mixes them with an air stream; the second group forms droplets from the liquid suspension which are dried to produce much the same effect (Schmoll et al., 2009). Examples of the first

group include acoustic dry aerosol generator/elutriators, fluidized bed aerosol generators, and a turntable/venturi aspirator system. The second group includes electrospray generators and Collison nebulizers. A study comparing 5 types of methods found the Collison nebulizer to be most consistent for nanoaerosol generation, though the other systems had advantages that would be situationally useful (Ibid.).

Once the aerosol is generated, there are several ways to characterize it. Metrics such as number of particles per volume of air, size distribution based on diffusivity diameter, and ratio of mass of the aerosol to air volume all aid in understanding the exposure created in the test chamber (Hinds, 1999). Essentially, developments in aerosol science allow the measurement and estimation of several exposure factors, which in turn can be compared to toxic effects observed in the exposed subject.

A variety of methods and instruments facilitate this characterization. Direct-reading instruments have the advantage of being convenient and immediate, but are used for different purposes from filter-based air sampling with lab analysis.

Specific Aims

In general, the research aimed to characterize both the exposures generated in the chamber and doses delivered to any hypothetical test organism.

Specific aims can be delineated under several headings:

Construction and testing of the apparatus as a whole;

Describing the total air concentration, size distribution and surface area of the salt carrier particles;

Quantifying the cadmium exposure to an organism placed in the test chamber;

Estimating the dose of cadmium that would infiltrate different areas of the respiratory tract of test animals.

Design and Methods

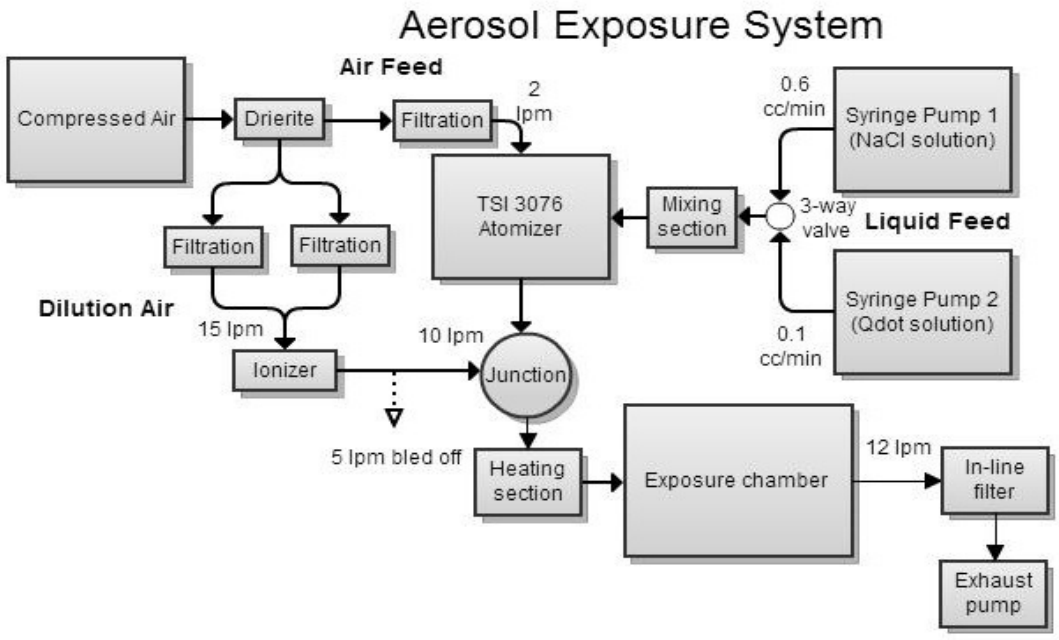

Figure 1: General Diagram of Exposure System

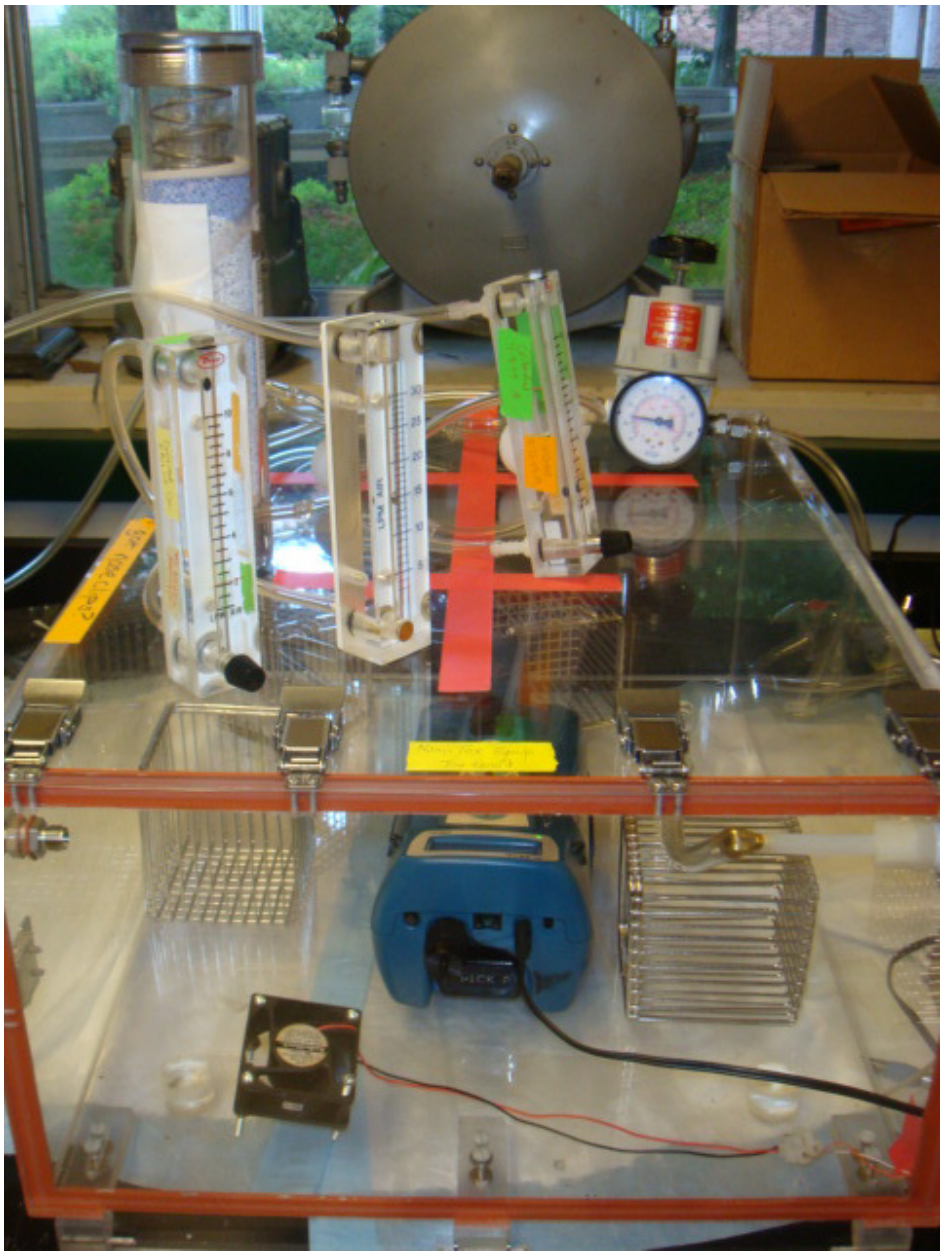

Figure 2: Photograph of Exposure System

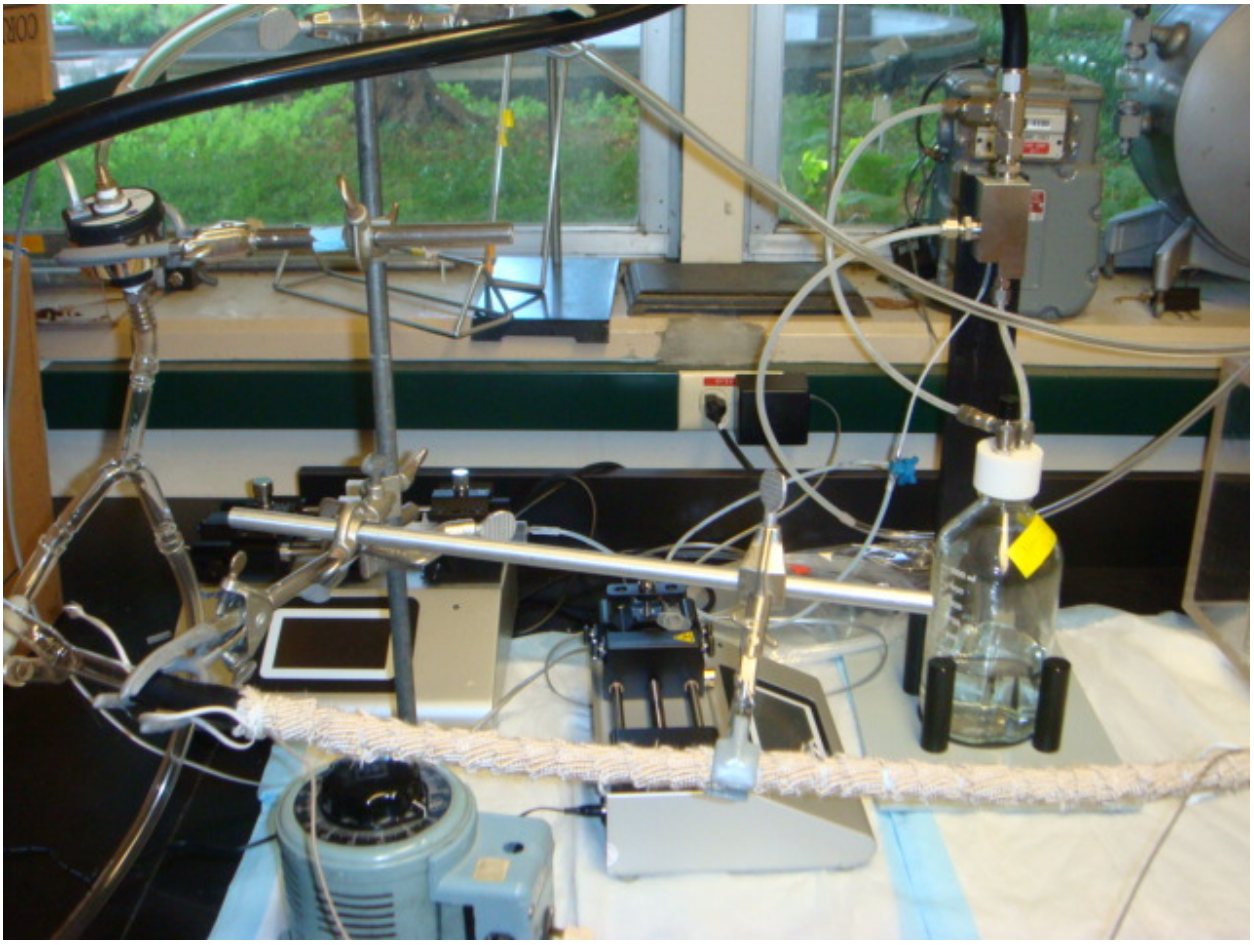

Figure 3: Photograph of Exposure System

Atomizer

The atomizer used was a TSI Model 3076 Constant Output Atomizer. Operating in the non-recirculation mode kept the concentration of the liquid feed constant, as excess liquid was simply collected in a jar. This is in contrast to recirculation mode, which does not remove this excess liquid from the feed, affecting the solution's properties over time.

Liquid Feed System

In preparation for the liquid feed, the carrier particle and Qdot solutions must be created. For the first, pure NaCl was mixed in with Milli-Q water at a ratio of 1 to 5 mg per 10 ml. In practice, larger volumes and masses (resulting in 100-200 ml of solution) were used to increase precision and to generate enough of a supply to enable extensive testing.

The size of the particles generated depends on the salt concentration in the liquid feed. The atomizer is stated to generate droplets with a number mean diameter of 350 nm. By using a more concentrated solution, the mass of salt remaining when the hypothetical droplet dries is also increased, resulting in a larger particle. The 0.1 mg/ml ratio suggested by the atomizer's manual was concentrated enough to reliably produce a high number of particles, while dilute enough to maintain a nanoscale size distribution.

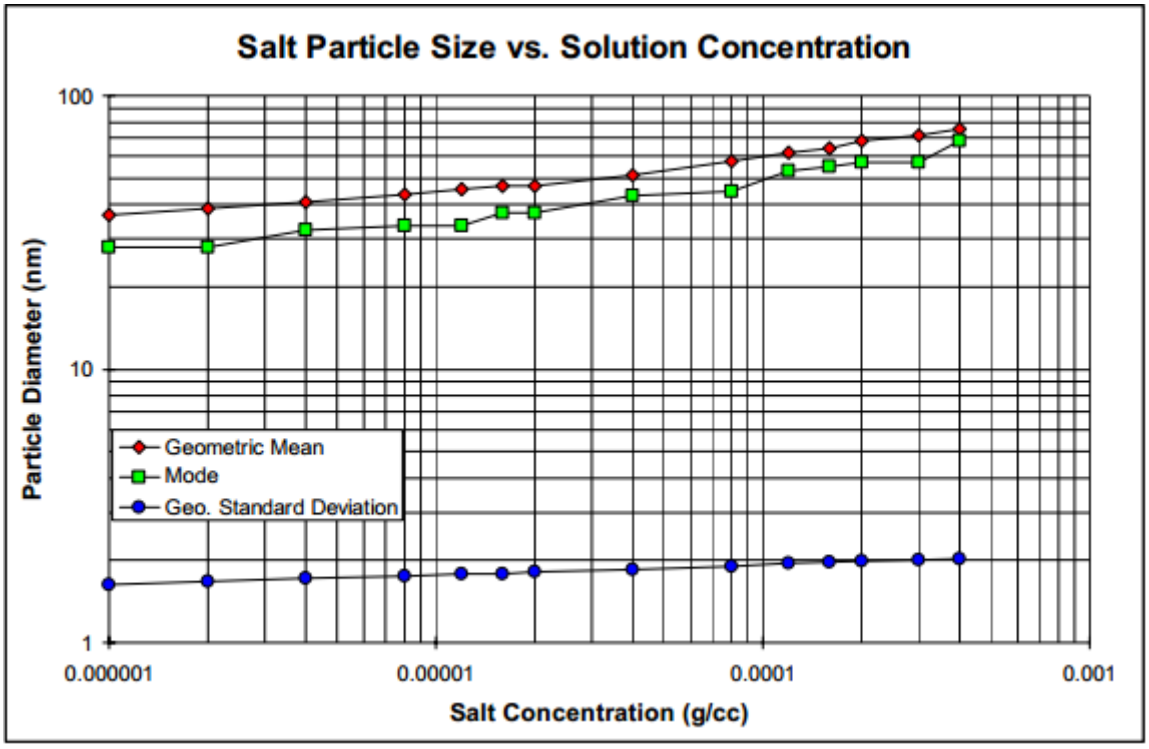

Figure 4: Salt Particle Size vs. Solution Concentration (from TSI, 2005)

The Qdot solution originally arrived from Professor Xiaohu Gao's lab by way of the Nanotoxicology Center. While the concentration of quantum dots was reported to be a generous 1 micromolar, the small volume (1.5 ml) necessitated dilution. To this end, 1 ml was added to 14 ml of Milli-Q water, creating 15 ml of about 0.07 μM solution. Furthermore, 1 ml of this diluted solution was added to 9 ml of Milli-Q water to make 10 ml of an even more dilute (7 nM) solution. This 7 nM solution was only used to prepare a spiked filter for ICP-MS analysis.

Two KDS syringe pumps provided the liquid feed for the aerosol. The larger of the two, a Legato 270 model, infused 0.6 mL/min of the NaCl solution. The smaller pump, a Legato 180 model, infused 0.1 mL/min of a

prepared Qdot solution. These two streams traveled to an adjustable three-way valve, where they then entered a thin mixing section of tubing. A length of corkscrew-shaped wire was ultrasonically cleaned then inserted into this mixing section, increasing the turbulence of the flow and allowing for greater combination of the two streams. The end of this tubing was attached to the liquid inlet on the atomizer.

Air Feed System

A laboratory compressed air valve was used as the air source. The compressed air flowed through a regulator to ensure that pressure did not exceed 35 psig, according to the atomizer manufacturer's recommendations. Next, it was dried using a Drierite laboratory gas dryer filled with anhydrous calcium sulfate. The gas line was split into two sections: the atomizer feed, and the dilution air stream (to be covered later). The atomizer feed was then purified with a small capsule filter (Pall 4210 Bacteria Air Vent hydrophobic glass laminate depth filter) and restricted to 2 lpm using a rotameter with a flow control valve. Finally reaching the atomizer, it combined with the liquid feed to produce aerosol.

Dilution Air

After the aforementioned split in the compressed air line, the dilution air was split again and filtered through two more Pall capsule filters to

reduce the loading on each one. Using another rotameter, the two streams were rejoined and restricted to 15 lpm, sufficient for the air ionizer next in the line. The air leaving the ionizer was split again in as short a distance as possible; one fork (10 lpm) combined with the aerosol stream leaving the atomizer, while the rest (5 lpm) was simply bled off to lower the total amount of dilution air and keep the ultimate air concentration of aerosol in the chamber as high as possible. Investigation with an ion counter confirmed that the air stream combining with the aerosol was sufficiently ionized to neutralize the final product.

Adding dry, bipolar ionized dilution air counteracted the intrinsic humidity and neutralized the electric charge of the particle stream leaving the atomizer. This was desirable, since charged particles would cause wall losses and wet particles could easily throw off the size distribution of the aerosol.

To add flexibility in controlling temperature, a heating section was attached directly after the point of combination. It consisted of a Teflon tube wrapped with heating tape, which was plugged into a variable-voltage transformer and adjusted to keep the relative humidity percentage a safe amount below NaCl's efflorescence point of roughly 40-50% (Gao et al., 2007). (In practice, efflorescence would occur more readily due to the Qdots providing nucleation sites for the NaCl.) The tube's diameter was purposefully kept small so as to enable rapid heating of the total stream

rather than the air closest to the tube walls. At the end of this heating section was the inlet to the exposure chamber itself.

Exposure Chamber and Exhaust

A clear acrylic box with a hinged door and two airstream ports was used for the exposure chamber. Roughly 150 liters in volume, it was large enough to allow instrumentation and test animals to be inserted, while small enough to minimize issues with incomplete mixing of air. To further encourage mixing, a small 12V fan was placed near the inlet and continuously operated during sampling. Lastly, a small extension to the exhaust port on the inside increased the distance from inlet to outlet, again with the intention of more even concentration throughout the entire chamber. Temperature and humidity conditions in the chamber while the atomizer was working were found to be optimal: 85 degrees Fahrenheit and 28% relative humidity.

Exiting the chamber was a length of tubing that had an in-line filter to capture any remaining particles. Since the filter restricted flow out of the chamber to an extent, a pump was placed at the end of the exhaust line and matched to the airflow at the inlet, pulling 12 lpm of air. This prevented leaking out of the chamber, while matching the two flow rates prevented infiltration of outside air into the chamber.

Chamber Evaluation and Particle Counting with P-Trak

In order to determine that the atomizer setup was working properly, direct measurement methods were employed. Assuming that the omission of quantum dots would not significantly alter the behavior or size distribution of the carrier particles, all direct measurement was carried out with the three-way liquid feed valve configured to let only the salt solution flow. Using a TSI P-Trak Ultrafine Particle Counter in the automatic logging mode, data was gathered about the presence of particles generated by the setup as well as the rise and decay of concentration over time. The instrument itself was placed near the entry point of the aerosol stream to increase sensitivity to the changing concentration; a previous master student's thesis (Kim 2010) attested to the lack of dead spots in this chamber, so evaluation in other sections was not performed.

In addition, the P-Trak combined with size-selective diffusion screens was used to construct a thermodynamic diameter size distribution of the salt particles generated. Since the P-Trak only reports a single number of all particles measured above 20 nm, it was necessary to use the screens to restrict the amount of particles that came through. By attaching a screen holder to the inlet port on the P-Trak, the minimum particle size cutoff was increased with an added quantity of screens in the holder, though the threshold was somewhat gradual, as seen on Graph 2. In contrast to the chamber evaluation, this was accomplished by taking single samples through

the screen holder while removing one screen at a time. The differences between multiple observations using variable numbers of screens corresponded to the histogram bins of the aerosol's size distribution.

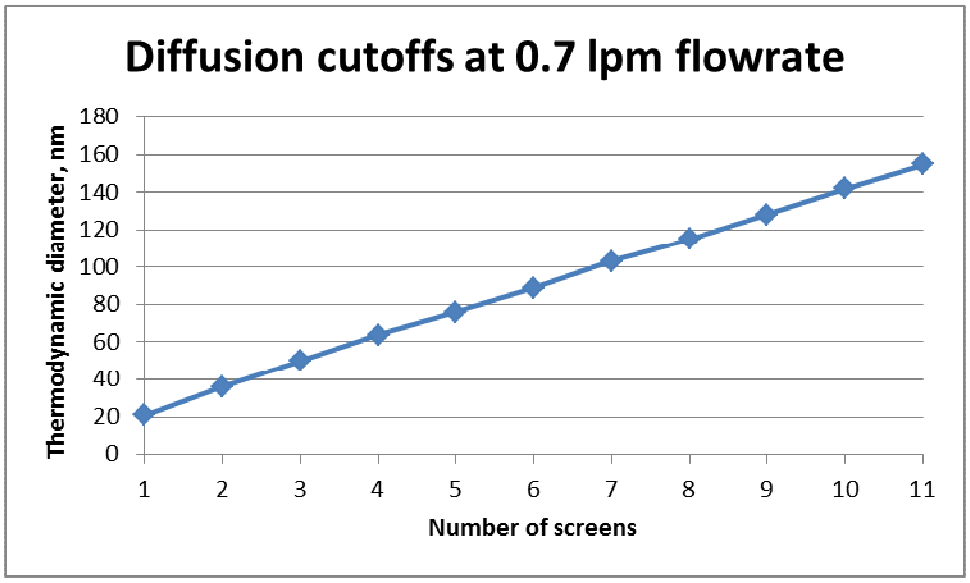

Graph 1: Thermodynamic Diameter Minimum Size Cutoffs Imposed by Diffusion Screens

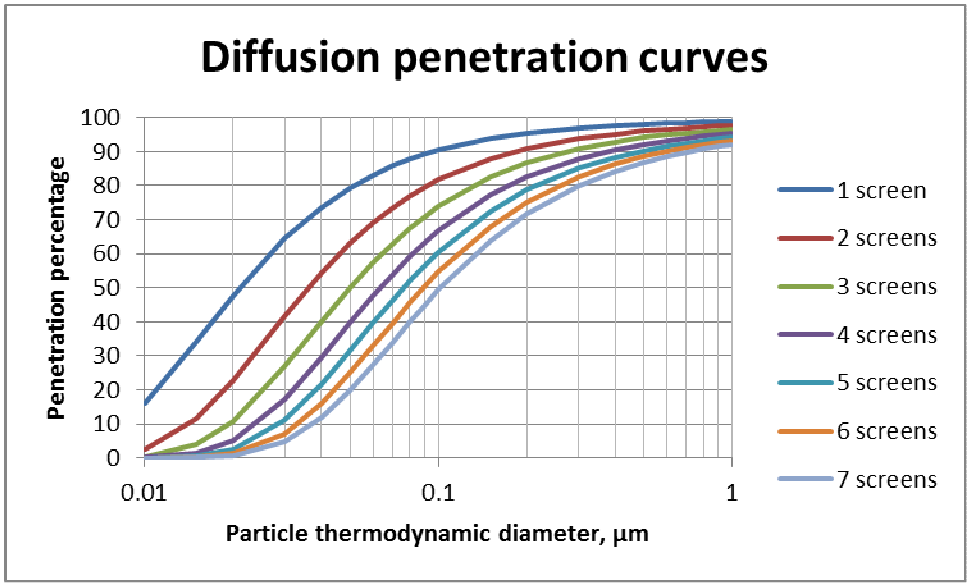

Graph 2: Penetration Curves Based on Number of Diffusion Screens and Particle Diameter

The frequent dilution of chamber air due to opening the chamber door and changing the number of screens in the holder caused problems with reproducibility of measurements. Initially, to combat this, sampling took place in the immediate region of the exposure chamber's inlet. This measurement had the disadvantage that the absolute number of particles would be vastly different in the chamber as a whole. For example, a measurement of 450,000 particles per cubic centimeter in the incoming stream would translate into a lower count per cubic centimeter in the breathing zone of an organism in the center of the chamber. In addition, measurements taken in the inlet area were still not satisfactorily consistent, and were frequently above the P-Trak's limit of detection of 500,000 particles per cubic centimeter. Lastly, the size distribution data found in this way had an overwhelmingly sharp peak in the smallest size bins, directly contradicting the atomizer manufacturer's indication that 0.1 mg/ml salt solution would generate an aerosol with a lognormal distribution around 60 nm.

Instead, a small secondary dilution chamber was constructed. This consisted of a metal foil-lined plastic box with four ports on it. One port served as an inlet for the aerosol. This setup reported consistent measurement values, and the dilution reduced the particle counts to within the limit of detection without affecting the size distribution. The concentration of the salt solution was also increased from 0.1 mg/ml to 0.5

mg/ml for these specific tests to shift the size distribution slightly higher in the detection range of the P-Trak and screens.

A Grimm 1.109 aerosol spectrometer and 1320 NanoCheck, direct-reading instruments with diameter detection ranges of 250 nm-32 micrometers and 25-300 nm respectively, were used to get more detailed data on both nanoscale and larger particles. Since the 1320 NanoCheck was only able to report a count mean particle diameter and total particle count, its results were interpreted in a looser, descriptive fashion for comparison with the P-Trak results. On the other hand, the 1.109 aerosol spectrometer provided a detailed 31-bin size distribution for larger (250 nm-32 micrometers) particles, and was thus taken as an authoritative measure of those optical diameter size categories.

Sampling Scheme

25mm polycarbonate track-etched filters were deemed to be the best for scanning electron microscopy. This was due to the filters' non-hygroscopicity and smooth surface, which produced favorable conditions for sputter coating and imaging. Pore size was relatively unimportant, as diffusion is the main vehicle for deposition of ultrafine particles (Hinds).

On the other hand, 37mm mixed-cellulose ester filters were used for ICP-MS analysis of the aerosol. Here, smoothness of the filter surface and moisture properties were less important, but the relative ease with which

MCE filters can be chemically digested was desirable.

These filters were loaded into cassettes and used, two at a time, for air sampling. In contrast to the configuration used with the P-Trak, the three-way liquid feed valve was set to allow both the saline solution and the quantum dot solution into the atomizer. The setup was run for 5 minutes before the two sampling pumps were set near the mixing fan and the first samples taken. Six samples (three of each type) were taken at 1.55 lpm for 10 minutes per sample; the chamber door was opened and the pumps removed at the end of each sampling period. A Bios Defender DryCal gas flow calibrator was used before and after each period to ensure less than 5% drift in the sampling rate. After all samples were taken, the chamber was flushed by switching off the syringe pumps, closing the three-way liquid feed valve, and allowing air to flow for an additional 15 minutes.

SEM Imaging, Counting by Fields, and Particle Surface Area

The polycarbonate filters were prepared for electron microscopy through sputter coating. After drying them using a sealed jar containing desiccant, they were cut into small pieces to be bound to an SEM stud with carbon tape. The studs were sputter coated using the University of Washington Nanotechnology User Facility's (NTUF) equipment with a 7 nm layer of gold and palladium, since the sample medium was not conductive enough on its own to allow for imaging.

For the purposes of taking electron micrographs, a variety of magnifications were used. The main goals were to get both a general idea of particle density and of the morphology of the particles themselves. For these purposes, 50,000 to 60,000x magnification was deemed to be sufficient.

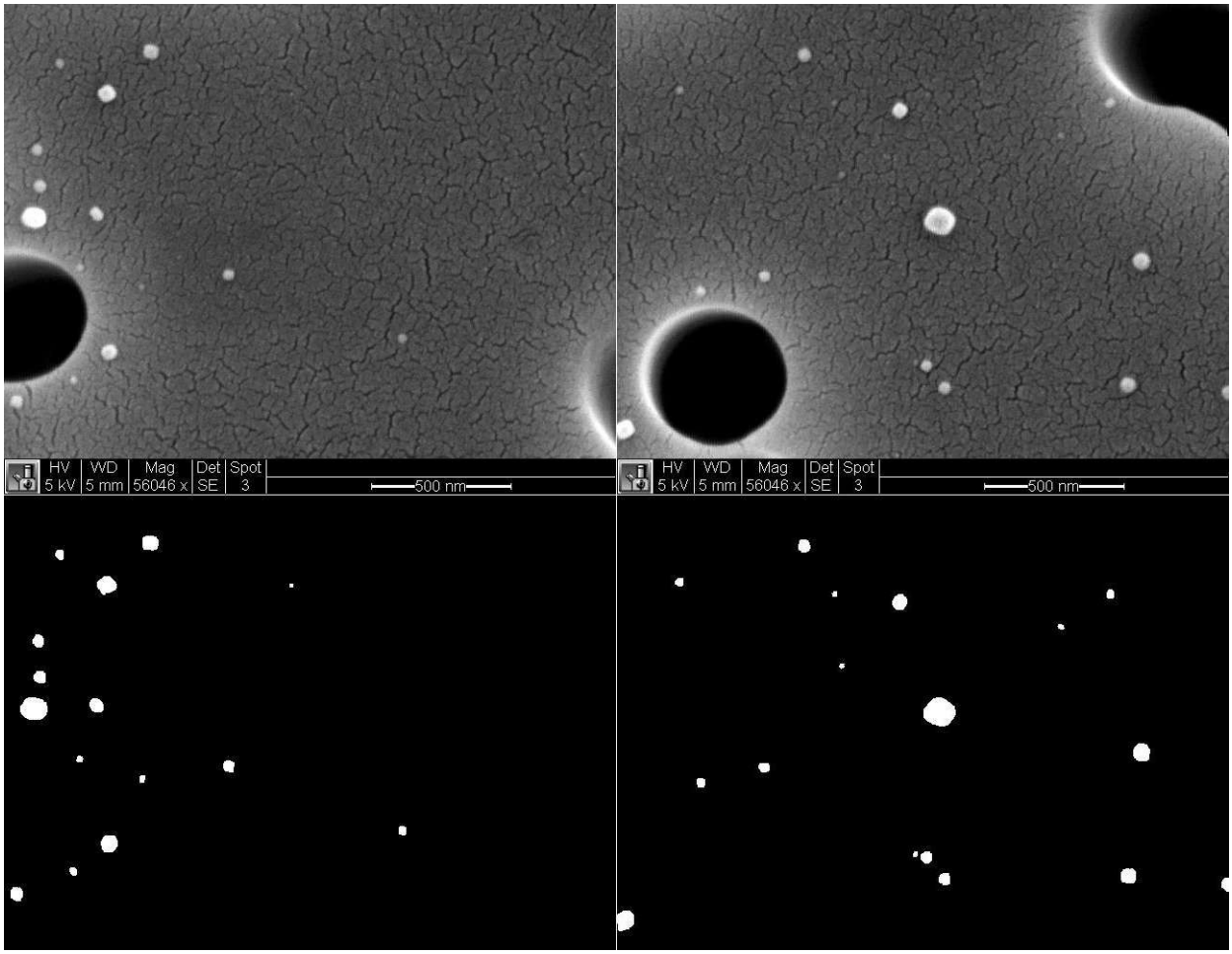

Figure 5: Sample SEM Fields and Corresponding Threshold Analyses

Images at these magnifications were also useful for counting by fields. The TIFF images from the SEM were imported into ImageJ software calibrated to have the correct tolerances for the particle sizes involved. After verifying its utility by manually counting a field and comparing it to

automatic counting, the program was used to count and measure particles in 20 fields from each of the three samples. While ImageJ did not automatically provide diameter information, the area measurements (A) were assumed to be roughly circular and related to a projected area diameter (d) using the equation $A = pi*(d/2)^2$. This data was then compiled into total particle counts and proportional size distribution and compared to the data obtained via the P-Trak.

Additionally, particle surface area (SA) was estimated, assuming roughly spherical particles ($SA = 4*pi*[d/2]^2$) whose cross-sections were shown on the micrograph. These estimations were compared to results from the direct-measurement AeroTrak 9000. The AeroTrak's operating principle relies on electrical detection of charged aerosol particles. The charge detected is proportional to the surface area, since greater particle surface area allows more air ions to cling to the particle. This tool was used to take samples of particle surface area per cubic centimeter of air, based on alveolar and tracheobronchial fractions of particle size. Since the AeroTrak was too large to fit inside the chamber, it was configured to sample directly from the incoming stream. This was in contrast to the polycarbonate filters, which sampled from within the chamber.

ICP-MS Analysis for Cadmium and Zinc Content

In addition to the MCE filter samples obtained previously, two spiked

filters and four laboratory blanks were necessary for calibration. The spikes were prepared by laying the filter on top of the opening of a clean flask, adding 0.1 ml of Qdot solution, and allowing to dry, placing a large beaker over it to keep air currents and dust from affecting the spike. The first filter spike used the same concentration as was used in the liquid feed; the second filter spike was from a solution with a tenth of the concentration. The laboratory blanks were simply removed using forceps from the filter package. All of these were placed inside plastic filter sample holders and delivered to the Environmental Health Laboratory.

Cadmium and zinc were chosen as the two analytes of interest for specific reasons. First and foremost, cadmium was the element with the most toxicological implications in the aerosol. Also, an estimate of the number of Qdots that reached the filter could be made, depending on the diameter of the dots and therefore their cadmium content per dot.

Zinc was chosen due to the composition of the dots themselves. Since the shell is made of zinc sulfide, zinc would also necessarily exist in the samples. The ratio of zinc to cadmium was assumed to be indicative of the size of the dots; smaller dots would have a greater proportion of their mass as part of the shell. As such, knowledge of the size of the dots used in the aerosol along with zinc and cadmium content could corroborate estimations of the total number of quantum dots in a sample. Also, as a general rule, multiple analytes allow for greater verification of the primary analysis.

Calculation of Dose Delivered to a Hypothetical Animal

The data obtained from ICP-MS analysis, direct particle counting and SEM particle counting were measures of exposure that could be used to estimate the dose inhaled by a mouse, given other parameters. These other parameters included items such as exposure duration, breathing rate, breathing volume, and animal weight. By integrating the graph obtained from the P-Trak chamber evaluation, it was possible to make a simple estimation of particles inhaled by a lab animal placed in the chamber from the start, rather than assuming that the air concentration of cadmium remained at steady state conditions during the entire exposure period.

Menache et al. (1995) suggested that small laboratory animals inhaled 95% of particles sized <0.7 micrometers. Since these were much larger than the particles generated by the atomizer in this apparatus, it was assumed that every particle in each volume of breath taken in by the animals was inhaled. Alessandrini et al. (2008) found that about 60% of ultrafine particles were deposited into the intrathoracic region, comprising the trachea, bronchial tree and alveoli. This was used for a rough "respirable fraction" calculation.

Results and Analysis

Chamber Evaluation and Particle Counting with P-Trak

Feed rate of NaCl, ml/min	0.6
NaCl concentration for chamber evaluation, mg/ml	0.1
Particles in incoming stream, pts/cc	500000
Maximum chamber concentration (15 min infusion), pts/cc	241050
Decay constant after infusion, minutes	4.4
Growth constant during infusion, minutes^-1	0.24
NaCl concentration for size distribution testing, mg/ml	0.5
Estimated median diameter by particle count, nm	89
Median by count excluding large particles (>103 nm), nm	76
Standard deviation of size distribution, estimated	87
SD excluding large particles	19

Table 1: Summary of P-Trak Evaluations

Maximum concentration within the chamber was measured and was found to be roughly half the concentration in the incoming aerosol stream. While 500,000 pts/cc was the upper limit of detection for the P-Trak, the reading fluctuated slightly below that number and previous sampling found a value of about 480,000 pts/cc.

The chamber's peak of 241,050 particles/cc was attained after 15 minutes of infusion. After that, the infusion stopped (though removal of air using the exhaust pump continued) and the decay time constant was calculated as -27/ln(536/241,000)=4.4 minutes. That is, the concentration is reduced to about 37% of its original value every 4.4 minutes.

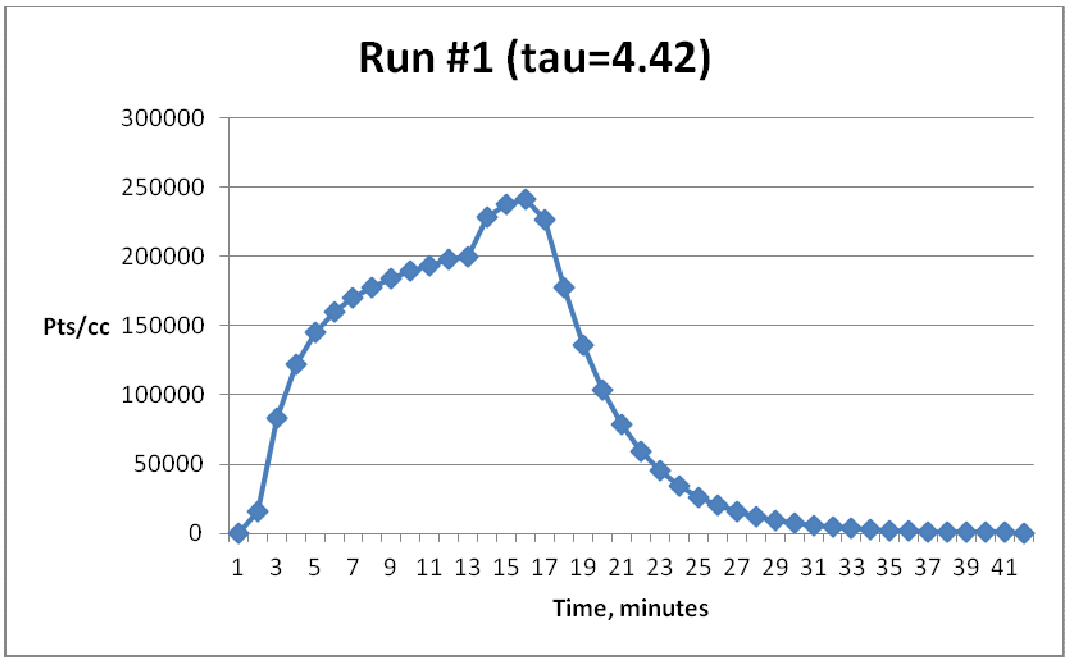

Graph 3: Particle Concentration over Time, Infusing for 15 Minutes and Decaying for 25 Minutes

Another run was performed where infusion lasted for 25 minutes. While this run's maximum (238,000 pts/cc) was achieved at the 25-minute mark, any significant change had long halted by then. There was less than 5% increase between samples at the 10-minute mark, and less than 1% after 20 minutes, with a sampling interval of 1 minute. Using this data, the growth constant k during the first 20 minutes of infusion was calculated as ln(227,250/1,795)/20 = 0.24.

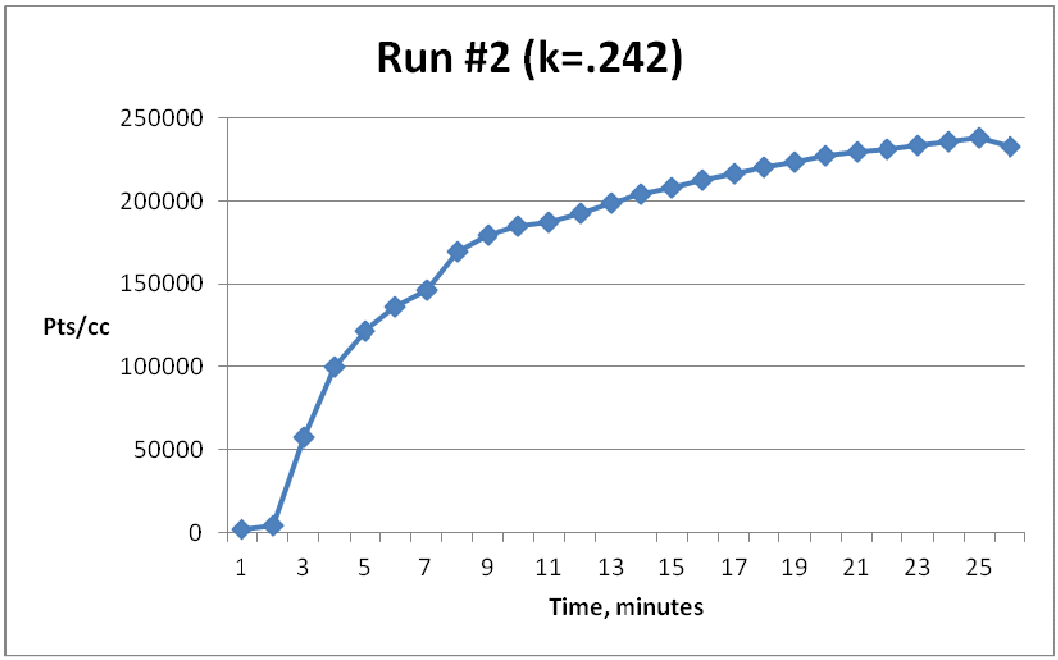

Graph 4: Particle Concentration over Time, Infusing for 25 Minutes

Thermodynamic diameter size distribution measurements were taken using two P-Traks sampling in parallel with diffusion screens. The two instruments reported comparable data: one had a mode at 64 nm, whereas the other had a sharper peak at 76 nm, the next size class. The largest size class (103 nm to 1 micron) has been omitted for clarity.

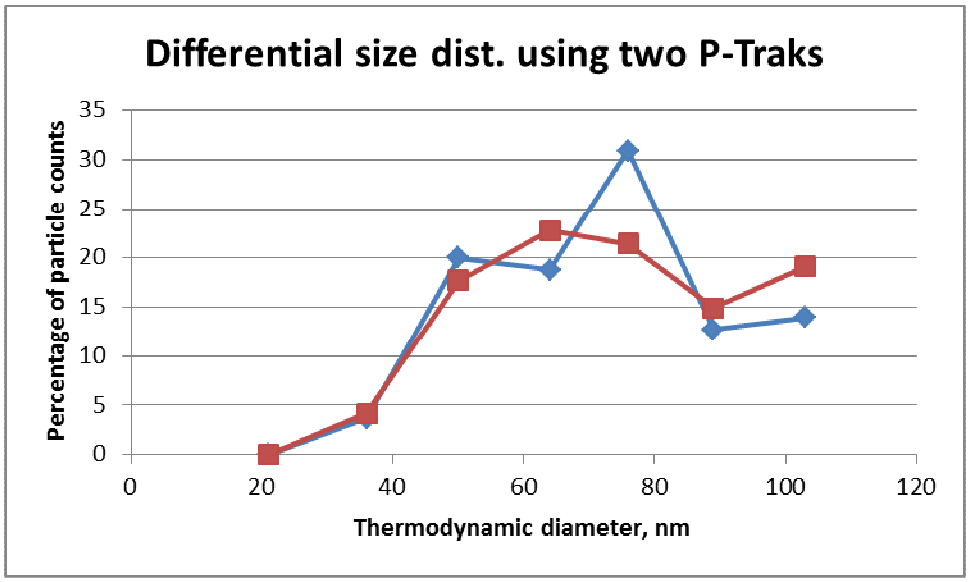

Graph 5: Differential Size Distribution of Particles as Measured by P-Trak and Diffusion Screens

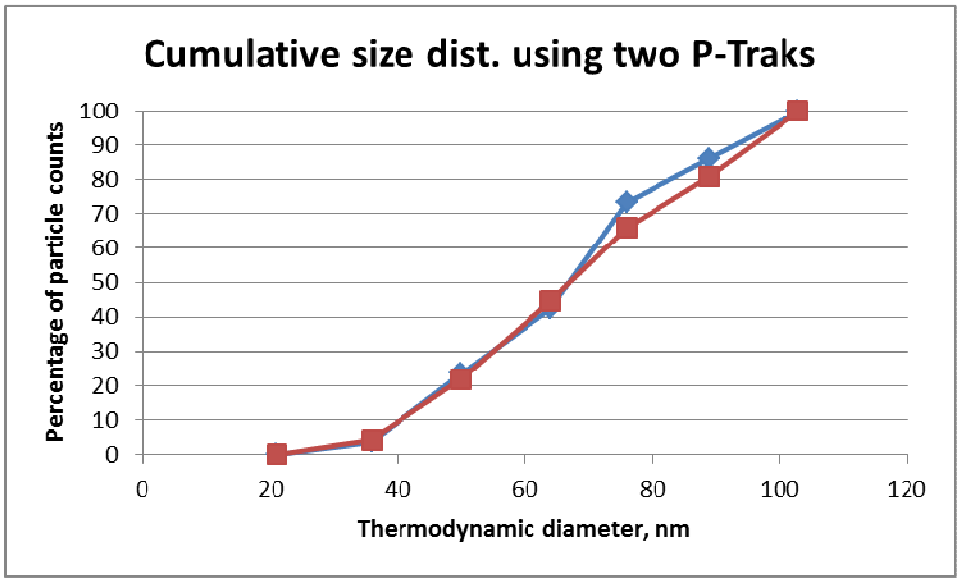

Graph 6: Cumulative Size Distribution of Particles as Measured by P-Trak and Diffusion Screens

The actual size distribution data was calculated based on manufacturer's recommendations for the Particle Size Selector. The P-Trak only gives a raw particle count, rather than a count based on size; placing the diffusion

screens in front of it prevents the smallest of particles from getting through, lowering the absolute count. For example, using 1 screen and the P-Trak's flowrate of 0.7 lpm, the minimum size cutoff is increased from 0.02 micrometers (imposed by the P-Trak itself) to 0.021 micrometers (imposed by the diffusion screen). By subtracting the difference between the reading with no screens to the reading with one screen, the number of particles in this size range can be found. The PSS manual contained a chart containing size cutoffs based on sampling flowrate and number of screens. From this, a series of equations to find cutoffs at other flowrates was derived. The cutoffs for variable numbers of screens at 0.7 lpm were used for this evaluation and entered into a spreadsheet to calculate differential and cumulative particle distributions.

The “Estimated median diameter” is based completely on particle count. Since a truly continuous description of each particle's size was not possible, the particles in each size range were assumed to be all as large as the 50% cutoff value. Thus, if there were 500,000 particles/cc total in the chamber, the estimated count median diameter is the size class containing the $250{,}000^{th}$ particle.

The Grimm instruments added to the data concerning the aerosol's size distribution across a broad range of diameters. The 1320 NanoCheck reported particle mean mobility diameters in the 30-40 nm range, in contrast to the P-Traks' 64-76 nm thermodynamic diameter range. The

1.109 aerosol spectrometer reported that very few particles (about 0.1% of the whole) had optical diameters larger than 250 nm, as was expected from the atomizer manufacturer's manual.

SEM Imaging, Counting by Fields, and Particle Surface Area

Sampling time per filter, minutes	10
Sampling rate, lpm	1.55
Fields counted per sample	20
Total particles counted	621
Estimated median diameter, nm	39
Mode, nm	35
Standard deviation	28.5
Total area of fields counted, um^2	228.9
Effective collection area per filter, mm^2	385
Derived air concentration, pts/cc	67400
Combined surface area of 621 particles, um^2	5.635
Derived surface area concentration in air, um^2/cc	612
AeroTrak surface area reading (alveolar fraction), um^2/cc	4265
AeroTrak surface area reading (tracheobronchial fraction), um^2/cc	1225

Table 2: Summary of SEM Evaluations

There was a significantly lower concentration of particles using the electron microscopy method compared to the P-Trak. Though the filter samples were taken in roughly the same region as the P-Trak's inlet port, the calculated amount of particles was one-fourth of the previously-obtained direct measurement numbers.

On the other hand, a histogram of the size distribution neatly fits into a lognormal shape. Again, this is distinct from the P-Trak and diffusion screens' results. Nearly half of the particles counted were placed into the

three bins of 21, 30 and 38 nm diameter, with 30 being the largest bin of all. The tail on the right end of the distribution causes some positive skewness, due to the counting of particles approaching 200 nm or more. Correspondingly, the arithmetic mean was disproportionately affected by outliers on the right end and was about 10 nm higher than the median. However, there is good agreement between the geometric mean and the median of the data set.

In terms of surface area, the ImageJ data was much lower than the AeroTrak 9000 reading for the alveolar fraction, while higher than the tracheobronchial fraction. Since the fractions are based on a continuous model rather than on specific size cutoffs, no further comparison of counted particles versus directly-measured surface area was performed.

An attempt was made to use the SEM's energy-dispersive X-ray spectroscopy (EDX) to quantify the amount of cadmium in the particles. However, since the load of cadmium was miniscule, especially in comparison to the other elements on the examined filters, it was undetectable by EDX.

ICP-MS Analysis for Cadmium and Zinc Content

	Standard/Average	**Maximum**
Feed rate of NaCl, ml/min	0.6	
Feed rate of Qdots, ml/min	0.1	
NaCl concentration, mg/ml	0.1	
Qdot concentration, #/ml	4.02E+13	

Sampling time, minutes	10	
Cd atoms per dot	3850	
Mass of Cd per atom, µg	1.87E-16	
Mass of Cd per dot, µg	7.1995E-13	
Cd concentration, µg/l	0.0011	0.0024 (sample 3)
Carrier particles according to P-Trak, #/cc	241050	
Cd per carrier particle, µg	4.56E-12	9.96E-12
Qdots per carrier particle	6.34	13.83
Qdot concentration, #/cc	1.53E+06	3.33E+06

Table 3: Summary of ICP-MS Evaluations

Qdot concentration, number of cadmium atoms per dot and all derived values are based on figures provided by the Nanotoxicology lab. As noted earlier, this means that the pure undiluted stock was assumed to be 1 micromolar Qdots; that the first dilution, used for the aerosol and one of the spikes, was a fifteenth of that; and that the second dilution, used for the other spike, was a tenth of the first. The range of cadmium atoms per dot was given as 3500 to 4200, leading to the assumption of 3850 on average.

Three samples were taken in succession. While all three samples agreed within an order of magnitude, the third sample was considered to be the most accurate representation of air concentration of quantum dots at steady state in the exposure chamber. However, the average air concentration between all three samples is shown above.

The two spikes, along with the cadmium content results on the spikes from the Environmental Health Laboratory, were used for a secondary analysis. This started with the 1 micromolar figure for the initial Qdot stock but attempted to find a more specific number of Cd atoms in each dot. The

assumption was made that the 0.1 ml of the first spike solution was exactly 1/15 micromolar, and thus contained

0.0001 l * 0.0667E-6 moles/l * 6.02E+23 dots/mole = 4.01E+12 dots.

The second spike contained 4.01E+11 dots, being 0.1 ml of a 10% dilution. The ICP-MS reports indicated 3.86 micrograms and 0.307 micrograms respectively of cadmium on the spikes. Applying the first concentration estimate, the amount of Cd atoms per dot was

3.86 µg Cd / (4.01E+12 dots * 1.87E-16 µg/Cd atom) = 5150 atoms/dot.

Applying the second concentration estimate, there were

0.307 µg Cd / (4.01E+11 dots * 1.87E-16 µg/Cd atom) = 4090 atoms/dot.

This results in an average of 4620 atoms/dot. Using this average in other calculations results in the following:

	Standard/Average	**Maximum**
Feed rate of NaCl, ml/min	0.6	
Feed rate of Qdots, ml/min	0.1	
NaCl concentration, mg/ml	0.1	
Qdot concentration, #/ml	4.02E+13	
Sampling time, minutes	10	
Cd atoms per dot	4620	
Mass of Cd per atom, µg	1.87E-16	
Mass of Cd per dot, µg	8.6394E-13	
Cd concentration, µg/l	0.0011	0.0024 (sample 3)
Carrier particles according to P-Trak, #/cc	241050	
Cd per carrier particle, µg	4.56E-12	9.96E-12
Qdots per carrier particle	5.28	11.52
Qdot concentration, #/cc	1.27E+06	2.78E+06

Table 4: ICP-MS Evaluations, Assuming 4620 Cd Atoms per Qdot

The net result of calculating Cd atoms/dot in this fashion is that an

aerosol with a lower concentration of Qdots is generated and that each carrier particle has fewer dots. The cadmium exposure remains constant.

Calculation of Dose Delivered to a Hypothetical Mouse

Data on respiratory rate and tidal volume are based on female BALB/c mice in Alessandrini et al. (2008) According to Menache et al. (1995), 95% of particles below 700 nm in size are at least inhaled, if not respired, by small laboratory animals. In accordance with this, an assumption was made that all particles generated at least entered the extrathoracic region, but that only ultrafine particles (<100 nm, corresponding to the smallest seven size classes in the P-Trak distribution data) could infiltrate the lower respiratory tract. This occurred at a rate of 60% (Alessandrini et al., 2008). The smallest seven size classes in the P-Trak data, ranging from 20 nm to 103 nm, comprised 62.3% of the total particle count. As a result, the "extrathoracic fraction" was (1 - 0.623) + (0.623 * 0.6) = 0.75, and the "intrathoracic fraction" was 1 - 0.75 = 0.25.

Using an exposure period of 30 minutes and assuming 3850 Cd atoms per Qdot:

	Standard/Average	**Maximum**
Carrier particles according to P-Trak, #/cc	241050	
Cd per carrier particle, µg	4.6E-12	1.0E-11
Air Qdot concentration, #/cc	1.5E+06	3.3E+06
Respiratory rate, breaths/minute	497	
Tidal volume, µl	229	
Minute volume, ml	113.81	

Total Qdot inhalation (30 min.), count	5.2E+09	1.1E+10
Total Cd inhalation (30 min.), µg	3.8E-03	8.2E-03
Ultrafine fraction (<103 nm)	0.623	
Fraction that remains in extrathoracic region	0.75	
Extrathoracic Qdot load (30 min.), count	3.9E+09	8.6E+09
Intrathoracic Qdot load (30 min.), count	1.3E+09	2.8E+09
Extrathoracic Cd dose (30 min.), µg	2.8E-03	6.2E-03
Intrathoracic Cd dose (30 min.), µg	9.4E-04	2.0E-03

Table 5: Hypothetical Dose at 3850 Cd Atoms per Qdot

With the same sampling period, but assuming 4620 Cd atoms/dot:

	Standard/Average	**Maximum**
Carrier particles according to P-Trak, #/cc	241050	
Cd per carrier particle, µg	4.6E-12	1.0E-11
Air Qdot concentration, #/cc	1.3E+06	2.8E+06
Respiratory rate, breaths/minute	497	
Tidal volume, µl	229	
Minute volume, ml	113.81	
Total Qdot inhalation (30 min.), count	4.4E+09	9.5E+09
Total Cd inhalation (30 min.), µg	3.8E-03	8.2E-03
Ultrafine fraction (<103 nm)	0.623	
Fraction that remains in extrathoracic region	0.75	
Extrathoracic Qdot load (30 min.), count	3.3E+09	7.1E+09
Intrathoracic Qdot load (30 min.), count	1.1E+09	2.4E+09
Extrathoracic Cd dose (30 min.), µg	2.8E-03	6.2E-03
Intrathoracic Cd dose (30 min.), µg	9.4E-04	2.0E-03

Table 6: Hypothetical Dose at 4620 Cd Atoms per Qdot

Discussion

Suitability of Chamber for Test Exposures

The fact that the chamber reaches a steady state concentration rapidly while the atomizer is operating is fortunate. Given that samples taken over ten minutes contained a significant amount of cadmium, reaching steady state at twenty minutes aids in further characterization and test exposures.

With a 50 ml syringe and using current flow rates, the NaCl solution syringe pump would be able to run for about another hour. With an alternating-syringe system, it would be possible to extend this indefinitely. In any event, the chamber's quick concentration growth is beneficial to any exposure study that takes place within.

Without any attachments, the inlet piece on the P-Trak is situated close to the surface it is placed upon. Whether it is low enough to make the reduced concentrations of aerosols near surfaces (Hinds 1999) an issue is debatable, but at the same time, the breathing zones of test animals would likely be at least as close as the inlet. As such, the data remain relevant.

Instrumental Measurement and Description of the Aerosol

One limitation on the data concerns the largest size category in the P-Trak size distribution. First, 103 nanometers to one micrometer comprises a vastly different range than any of the other size categories. Second, the upper limit of detection was taken from the manual, which also implies that particles even larger than a micrometer may be counted. On the other hand, data from the Grimm 1.109 aerosol spectrometer indicated that less than 0.1% of total particle counts were larger than 250 nm, so the 103 nanometer-1 micrometer range is, for practical purposes, 103 to 250 nanometers.

The discrepancy between the NanoCheck data and P-Trak data

illustrates an important point. The P-Trak is a condensation particle counter and measures thermodynamic diameter using diffusion screens. On the other hand, the NanoCheck uses electric conductivity to perform its readings, measuring mobility diameter. Depending on factors of the particles such as density and shape, the less these measurements will agree. Still, since almost all particles generated would be in the nanoscale regardless of which set of measurements is correct, the aerosol generator maintains its utility for nanoparticle test exposures.

Early size distribution testing reported unusual results, though after changing the sampling protocol, these phenomena were greatly reduced. The aerosol appeared to have a normal size distribution with the exception of an enormous peak in the smallest size bin. Since multiple tests with the P-Trak (n=6) showed the same pattern of unusual distribution, it is highly unlikely that it was due to chance. Furthermore, it contradicted the atomizer's manual, which suggests that a 0.1 mg/ml salt solution should produce a lognormal distribution with a geometric mean of approximately 60 nm. After changing the sampling point from the chamber inlet to a smaller dilution box, using different P-Traks, and increasing the salt solution's concentration to roughly 0.5 mg/ml, the results above were noted.

While the two P-Traks used for the final size distribution measurements obtained comparable data, there still was an appreciable difference in certain size categories and in total number of particles measured. It is reasonable

to assume that this was the result of an error in calibration. Additionally, since electrical noise within the instrument itself can drastically affect counts, such electronic issues may have contributed to the disparity.

A last point of interest regards the importance of dose measures in nanotechnology. In regulations, particulate matter and fumes are restricted according to mass concentration (e.g., $\mu g/m^3$). However, this paradigm is less effective with nanomaterials. For example, probably due to a larger surface area to volume ratio as well as increased surface reactivity, TiO_2 and carbon black nanoparticles are more injurious to lung tissue compared to their barely-reactive bulk materials (Nel et al.). As such, measures like mass median aerodynamic diameter (MMAD), while helpful for fine and coarse particles, become less helpful when dealing with nanoparticles. As a more detailed picture of the effects of individual materials forms, number-based rather than mass-based size distributions may be the most feasible way of determining risk from a nanoparticle-containing atmosphere.

SEM Imaging, Counting by Fields, and Particle Surface Area

There were considerable differences between data collected from direct measurement and from SEM imaging. Specifically, the particle counts obtained from analyzing the micrographs were far less than were measured with any other tool. The largest factor in the apparent lack of particles on the SEM filters is likely the fact that the filter pores are much longer

proportionally than they appear on the micrographs. According to the manufacturer, the thickness of the polycarbonate filter is approximately 10 to 20 micrometers, which is massive compared to particles in the nanoscale. Since the particles are found in higher quantity near the pores on the micrographs, it is reasonable that more particles deposited into the tunnel-like pores, and are unseen by the SEM, which only shows the surface. While this is the most compelling hypothesis to explain the disparity, other possibilities can be classified into measurement tool-related and SEM-related factors.

Due to the fewer levels of complexity involved in using direct-measuring techniques, there are probably relatively few factors of the observed errors that arose from their use. The most salient point to consider is the different type of diameters measured between the P-Trak and SEM analysis. As noted before, the P-Trak with diffusion screens measures the thermodynamic diameter, whereas counting by fields resulted in a projected area diameter. It is not unreasonable that these would be different for a given particle, and thus the entire size distributions measured by these two methods would also be significantly different.

Besides the P-Trak, the AeroTrak 9000 had dramatically different results from estimating surface area from counted particles. This is probably due to sampling with the AeroTrak in the immediate region of the chamber inlet rather than in the chamber proper (which would have fewer particles

and thus less surface area), as with the SEM samples. Also, the readouts were not a "total surface area" as was produced from the SEM images, but instead were different fractions of the surface area dependent on the ICRP model of lung deposition. All things being equal, the sum of these two fractions would be slightly less than the total surface area of all particles in the same volume of air.

The various techniques used in preparing and analyzing the SEM samples were another possible source of error and bias. Sputter coating may have "buried" some particles, making them difficult to distinguish. As can be seen in the micrographs, the coating appears as a flaky crust-like landscape, which occasionally produces points that are brighter than the surrounding area, but may just be imperfections in the surface. Since marking particles for counting was mostly done manually, some points that actually were particles may have been passed over to avoid false positives. The electron microscope has a reported resolution of 1-3 nm under ideal conditions, but these conditions are almost certainly dependent on the composition of the sample and the skillful adjustment of focus and stigmation. Smaller particles could be blurred into obscurity, especially at the magnifications considered. Likewise, due to the nature of the filter being used, particles tended to accumulate near pores. The pore edges were also bright enough to "wash out" some particles and make it difficult to distinguish the exact boundaries of others. If the filter used had a lower

porosity or larger pore size, this issue may have been mitigated. Even so, counting by fields has an inherent tendency to be unrepresentative of the actual air concentration and size distribution of particles. For example, as with asbestos fibers, fields may be picked from an area of a sample that has a randomly high number of comparatively large (or small) particles. This is tempered by the use of a high number of fields, but still, this random chance is a limitation to the method. Lastly, the assumptions of circular and spherical particles, for calculating diameter and surface area respectively, introduced some bias into the results. For instance, a noncircular particle would have a true diameter larger than the circle with the same area; and a nonspherical particle would have more surface area than a particle with the aforementioned circle as a cross-section.

Had the samples' composition been high enough to analyze cadmium content with EDX, it would have characterized the aerosol even further. For instance, it would allow the size distribution of cadmium to be estimated, as well as cadmium mass per particle. This is something to keep in mind for the future, though the amount of Qdots needed to load a sample with a detectable level of cadmium might be unfeasible from an economic standpoint.

ICP-MS Analysis for Cadmium and Zinc Content

The cadmium content from sample to sample appeared to validate the

assumption that taking samples in succession would show an increase until the chamber concentration stabilized. The "maximum" or third sample probably represents the most realistic exposure, given the fact that the first two samples were taken shortly after infusion began. Opening the door to change the filter cassettes likely also affected concentrations, creating a gradient that caused particles to flow from the inside of the chamber (far from the door) to the sampling area again. As such, if steady state concentration had been achieved deep inside (as probably happened by the time of the third sample), then there would be sufficient particles to create a near-maximum concentration in the sampling area. In the first two samples, steady state had not been achieved throughout the chamber, leading to a lack of enough particles to compensate for the door opening. A method of changing cassettes and checking pump flowrates without causing severe changes to the atmosphere inside the exposure chamber would alleviate this issue, allowing for more predictable test conditions.

Furthermore, in the liquid flow system, the slow trickle of 0.1 ml per minute of Qdot solution may have been insufficient. On occasion, the liquid in the tubing would be separated by "bubbles," causing variation in the amount that reached the atomizer. It remains to be seen whether using a higher flowrate with a more dilute solution would produce similar results in terms of dose. This brings up the issue of whether to reduce the saline flow rate to keep the total liquid flow rate constant or to increase it to retain the

NaCl molarity of the aerosolized solution. Similarly, another limitation of this study is that only one dilution of quantum dot solution was used in generating the aerosol. This raises the question of how correlated the concentration and feed rate are with the final amount of dots and cadmium that reaches the samples or organisms in the chamber. If this relationship were adequately described, studies with severe but extended inhalation exposures would be possible; as it is, the amount of quantum dots in the aerosol may be unsuitable for some experimental designs. Another possible relationship to explore would be the concentration and feed rate compared to the size distribution of the generated aerosol.

Oddly enough, though a proportional relationship between cadmium concentration and zinc concentration was expected, no such relationship was observed. Zinc may be an unsuitable tracer for cadmium in these quantum dots, despite the fact that the shells are made of ZnS, for a few reasons. One possibility is that the analytical method simply isn't sensitive enough for the low levels of zinc involved. Another is that the shells may be of variable thickness, geometry and surface area, meaning that CdSe cores of the same size may have vastly different shells in terms of zinc content. One way to investigate these issues would be to perform the same analytical method on a sample with a much higher Qdot content, preferably with homogeneity of core size by fabrication or as measured by emission wavelength. If a reliable correlation exists, then zinc could be used as a tracer in scenarios

with longer exposure periods or a higher level of quantum dots in the aerosol. The best way to sidestep the entire issue, however, would be to use an independent and easily-traced material like rubidium chloride. Simply adding a known amount to the liquid feed would suffice for the purpose of accurately detecting the cadmium in a sample.

By using the P-Trak diffusion screens with ICP-MS, it may be possible to get a thermodynamic diameter size distribution of cadmium content. Each individual screen could be washed, and the washing liquid analyzed using ICP-MS. The resulting data could be correlated with the known cutoff points for each screen to determine if Qdots preferentially combine with smaller or larger carrier particles. To achieve sufficient loading of dots, and therefore cadmium, on each screen, it would likely be necessary to run the aerosol generation system for longer or increase the Qdot solution's concentration above what was done in this research. Testing indicated that the second diffusion screen size category, 36 nm, received about 4 percent of particles, the lowest percentage of all the categories with a significant particle count. Given a .01 µg/L limit of detection for cadmium using ICP-MS and assuming that washing is performed with 100% extraction in 100 mL of liquid, minimum sampling time is estimated to be

.001 µg / (.04 x 241050 pts/cc x 700 cc/min x 4.6E-12 µg Cd/particle)

= 32 minutes.

Naturally, in practical application it would be prudent to use a much

longer exposure period to be doubly sure that enough cadmium-containing particles are loaded onto the screens.

Calculation of Dose Delivered to a Hypothetical Mouse

This system as configured is useful for creating medium-term, subacute inhalation exposures for small animals. This allows for a more generally realistic dosing situation: rather than simply injecting all of the Qdots at once or spraying a few droplets of highly-concentrated solution into the upper respiratory tract, the different toxicological effects brought on by a lower level of exposure for a longer period of time can be studied. As noted above, adding more syringes to the liquid feed system could allow for even longer exposure periods. This type of system could also be adapted for chronically exposing cell cultures as well, allowing for changes over time in the cells to be observed. In this case, the interior of the exposure chamber would be dramatically different both structurally and in terms of environmental conditions like temperature and humidity to ensure the cells' viability.

One potential issue lies in the fact that organisms require a certain balance of ions, and as such may reject the salt particles if this balance is disrupted. This would certainly be a problem for the bioimaging injection of Qdots in a saline solution—if the molarity of NaCl is too different from the body's, it will be rejected. On the other hand, with an inhalation exposure

and especially the exposures generated in this study, the mass of salt was likely too small to cause a significant change in the ion concentration in the hypothetical mouse's body. Still, this sort of question would warrant investigation if cell cultures were the target organism instead.

Summary

An atomizer was used to create a test aerosol of NaCl particles seeded with CdSe quantum dots in a small box-shaped exposure system. Using direct measuring tools, scanning electron microscopy and ICP-MS analysis of air samples, the exposure characteristics of the aerosol were determined. The results show that this chamber could be used to deliver a certain dose to an experimental organism for the purposes of toxicological study.

Works Cited

Alessandrini, F., et al. "Total and Regional Deposition of Ultrafine Particles in a Mouse Model of Allergic Inflammation of the Lung." *Inhalation Toxicology* 2008 20:6, 585-593.

Kim, C. "Nasal Inhalation Exposure Method of Quantum Dots to Mice using a Nebulizer." M.S. Thesis 2010. University of Washington: United States.

Derfus, A. M., W. C. W. Chan, and S. N. Bhatia. "Probing the Cytotoxicity of Semiconductor Quantum Dots." *Nano Letters* 2004 4:1, 11-18. Print.

Gao, Y., S. B. Chen, and L. E. Yu. "Efflorescence Relative Humidity of Airborne Sodium Chloride Particles: A Theoretical Investigation." *Atmospheric Environment* 2007 41:9, 2019-2023. Print.

Hines, M. A., and P. Guyot-Sionnest. "Synthesis and Characterization of Strongly Luminescent ZnS-Capped CdSe Nanocrystals." *Journal of Physical Chemistry* 1996 100:2, 468-71. Print.

Hinds, W. C. Aerosol Technology: Properties, Behavior, and Measurement of Airborne Particles. Wiley, John & Sons, Incorporated, January 1999.

Jamieson, T., et al. "Biological Applications of Quantum Dots." *Biomaterials* 2007 28:31, 4717-32. Print.

Menache, M.G., Miller, F.J., and Raabe, O.G. "Particle Inhalability Curves for Humans and Small Laboratory Animals." *British Occupational Hygiene Society* 1995 39:3, 317-328.

Nel, A., et al. "Toxic Potential of Materials at the Nanolevel." *Science, New Series* 2006 311:5761, 622-627.

Schmoll, L. H., et al. "Nanoparticle Aerosol Generation Methods from Bulk Powders for Inhalation Exposure Studies." *Nanotoxicology* 2009 3:4, 265-275.

TSI. Model 3076 Constant Output Atomizer Instruction Manual. Revision J,

June 2005.